

Torque-Ripple Minimization in Modular Permanent-Magnet Brushless Machines

Kais Atallah, Jiabin Wang, *Member, IEEE*, and David Howe

Abstract—This paper discusses the suitability of four-phase, five-phase, and six-phase modular machines, for use in applications where servo characteristics and fault tolerance are key requirements. It is shown that an optimum slot number and pole number combination exists, for which excellent servo characteristics could be achieved, under healthy operating conditions, with minimum effects on the power density of the machine. To eliminate torque ripple due to residual cogging and various fault conditions, the paper describes a novel optimal torque control strategy for the modular permanent-magnet machines operating in both constant torque and constant power modes. The proposed control strategy enables ripple-free torque operation to be achieved, while minimizing the copper loss under voltage and current constraints. The utility of the proposed strategy is demonstrated by computer simulations on a four-phase fault-tolerant drive system.

Index Terms—Fault tolerant, modular machines, optimal control, permanent-magnet machines, servo drives.

I. INTRODUCTION

BRUSHLESS permanent-magnet servomotors are increasingly being used in a variety of applications due to their high power density, high efficiency, and excellent dynamic performance as compared with other motor drive technologies. However, the presence of torque ripple in brushless permanent-magnet motors is often a major concern in applications where speed and position control accuracy is of great importance. Conventional three-phase permanent-magnet brushless servo motors embody design features such as distributed windings and/or stator/rotor skew, in order to minimize the cogging torque and harmonics in the induced electromotive force (EMF) [1]–[4], which result in increased manufacturing costs and reduced efficiency and power density. Furthermore, for applications where in addition to good servo characteristics, a degree of fault tolerance is also required, conventional brushless servo motors, would not meet the reliability requirements.

Modular permanent-magnet brushless machines, Fig. 1, differ significantly from conventional brushless machines, in that only alternate stator teeth carry a wound coil, which is conducive to low-cost, high-volume manufacturing, for applications in, for example, the automotive market, where a three-phase modular design is preferred and the machine can be driven by a conventional three-phase inverter. In addition, since the phase windings are es-

Paper IPCSD 03–100, presented at the 2003 IEEE International Electric Machines and Drives Conference, Madison, WI, June 1–4, and approved for publication in the IEEE TRANSACTIONS ON INDUSTRY APPLICATIONS by the Electric Machines Committee of the IEEE Industry Applications Society. Manuscript submitted for review March 26, 2003 and released for publication July 28, 2003.

The authors are with the Department of Electronic and Electrical Engineering, University of Sheffield, Sheffield S1 3JD, U.K. (e-mail: k.atallah@shef.ac.uk; j.b.wang@shef.ac.uk; d.howe@shef.ac.uk).

Digital Object Identifier 10.1109/TIA.2003.818986

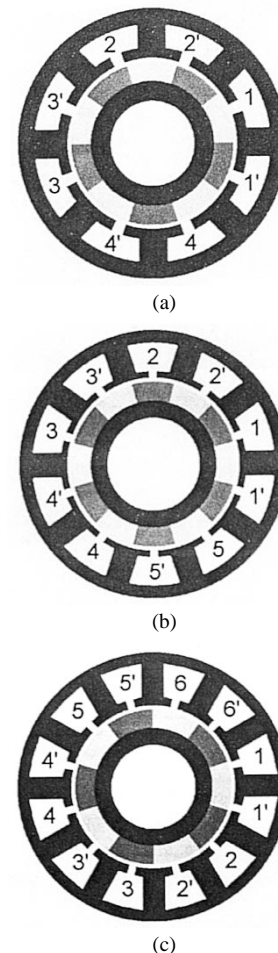


Fig. 1. Schematics of modular fault-tolerant machines. (a) Four phase. (b) Five phase. (c) Six phase.

entially isolated, magnetically, thermally and physically, their fault tolerance is significantly higher [5]–[7].

Furthermore, for a given number of phases, a relatively large number of combinations of stator slots and rotor poles exist [8].

Generally, it is assumed that modular machines have a sinusoidal back-EMF waveform, so that the current controller is required to track a set of sinusoidal current commands proportional to a given torque demand. However, this simple control strategy inevitably results in an undesirable torque ripple during normal operation if the back-EMF waveform is nonsinusoidal, and a large torque pulsation under a fault condition, such as an open-circuited or a short-circuited phase. While this problem may be partly overcome by adopting an optimal torque control strategy which is aimed at minimizing the copper loss when delivering the required torque demand [11]–[13], the effectiveness of existing strategies is limited by the available converter

voltage, since, by minimizing the copper loss, the resulting current command tends to be in phase with the back EMF. Consequently, at high speed the controller cannot track the commanded currents due to the limited converter voltage.

Many safety critical applications require a fault-tolerant drive to operate over a wide speed range, encompassing both constant torque and constant power operating modes. However, although, theoretically, a fault-tolerant brushless machine with one per unit inductance should be able to operate over an infinitely wide constant power region [14], existing control methods do not provide an effective means of facilitating such operation under both normal and faulted conditions. As a result, the potential power capability of modular machines is significantly compromised.

This paper discusses the suitability of four-phase, five-phase, and six-phase modular machines, for use in applications where servo characteristics and fault tolerance are key requirements, when a conventional sinusoidal phase current excitation is employed. It is shown that an optimum slot number and pole number combination exists, for which excellent servo characteristics could be achieved, under healthy operating conditions, with minimum effects on the power density of the machine. However, since a phase short-circuit or open-circuit fault, will result in significant torque ripple, the paper also describes a generalized optimal torque control strategy, applicable to both constant torque and constant power operating regions, and enables a ripple-free torque to be produced under healthy and faulted conditions.

II. EMF HARMONIC DISTORTION AND COGGING TORQUE

A. EMF Harmonics

In brushless ac servomotors, with sinusoidal phase current waveforms, harmonic distortion in the EMF and cogging are the two main sources of ripple in the output torque, and several techniques, such as winding distribution and rotor/stator skew are employed, in order to achieve sinusoidal EMF waveforms and reduce cogging.

For a healthy m -phase machine, the electromagnetic torque is given by

$$T_e(t) = \frac{1}{\Omega} \sum_{j=1}^m \sum_n \left\{ I_m E_n \sin \left(p\Omega t - \frac{2\pi j}{m} \right) \times \sin \left[n \left(p\Omega t - \frac{2\pi j}{m} - \phi \right) \right] \right\} \quad (1)$$

where I_m is the peak phase current, Ω is the speed of the motor, p is the number of pole pairs of the permanent magnets, and E_n is the amplitude of the n th EMF harmonic. Since there are no even-order harmonics in the air-gap flux density distribution due to the permanent magnets, n is a positive odd number. Equation (1) can be written as

$$T_e(t) = \frac{I_m}{2\Omega} \left(\sum_{j=1}^m \sum_n E_n \left\{ \cos \left[(n-1)p\Omega t - (n-1)\frac{2\pi j}{m} - n\phi \right] - \cos \left[(n+1)p\Omega t - (n+1)\frac{2\pi j}{m} - n\phi \right] \right\} \right). \quad (2)$$

Thus,

$$T_e(t) = \frac{m I_m E_1}{2 \Omega} \cos(\phi) + \frac{I_m}{2 \Omega} \times \left(\sum_{j=1}^m \sum_n E_n \left\{ \cos \left[(n-1)p\Omega t - (n-1)\frac{2\pi j}{m} - n\phi \right] - \cos \left[(n+1)p\Omega t - (n+1)\frac{2\pi j}{m} - n\phi \right] \right\} \right) \quad (3)$$

for $n = km \pm 1$.

Therefore, an EMF harmonic of order n contributes to the generation of torque ripple only if $(n \pm 1) = km$, where k is an integer. Thus, the EMF harmonics, which interact with the sinusoidal phase current waveforms to generate torque ripple, are as follows:

- $n = 5, 7, 11, 13, 17, 19, 23, \dots$, for a three-phase machine;
- $n = 3, 5, 7, 9, 11, 13, 15, 17, 19, 21, \dots$, for a four-phase machine;
- $n = 9, 11, 19, 21, \dots$, for a five-phase machine;
- $n = 5, 7, 11, 13, 17, 19, 23, \dots$, for a six-phase machine.

Consequently, for a four-phase machine all EMF harmonics will contribute to the generation of torque ripple, and conversely, for a five-phase machine only the higher order EMF harmonics, which are of small/negligible magnitude, generate torque ripple.

B. Slot Number and Pole Number Combination

In addition to other design parameters, such as magnetization distribution, slot opening, air-gap length, pole-arc-to-pole-pitch ratio, etc., the slot number and pole number combination of a particular design represents a good indication of its cogging performance. Recent work by the authors [8] showed that for a given number of phases of a modular machine a large number of feasible pole number and slot number combinations exist. Table I shows the smallest common multiple, N_c , of the number of slots, N_s , and the number of poles, $2 \times p$, and the optimal pole-arc-to-pole-pitch ratio for minimizing the fundamental component of cogging torque [10] (neglecting the fringing magnet flux into the slots), $\alpha_0 = ((N_c/2p) - 1)/(N_c/2p)$, of feasible one coil per phase modular machine variants. It can be seen that a large number of design variants exist, and it can also be seen that for most design variants, the optimal pole-arc-to-pole-pitch ratio is relatively large.

III. DESIGN VARIANTS OF MODULAR MACHINES

Fig. 1 shows schematics of a four-phase, a five-phase, and a six-phase modular fault-tolerant permanent-magnet brushless machine, respectively, which have been designed to meet the specification requirement of an electromechanical actuator for the more-electric aircraft. The three machines are equipped with parallel-magnetized $\text{Sm}_2\text{Co}_{17}$ permanent-magnet arcs,

TABLE I
SMALLEST COMMON MULTIPLE OF THE NUMBER OF SLOTS AND THE NUMBER OF POLES, AND OPTIMAL POLE-ARC-TO-POLE-PITCH RATIO (IN BRACKET)

	Number of phases m ($N_s = 2 \times m$)				
	3	4	5	6	7
	Number of rotor pole-pairs p	2 12 (0.67)	-	-	-
	3 -	24 (0.75)	-	-	-
	4 24 (0.67)	-	40 (0.80)	24 (0.67)	-
	5 30 (0.67)	40 (0.75)	-	60 (0.83)	70 (0.86)
	6 -	-	60 (0.80)	-	84 (0.86)
	7 -	-	70 (0.80)	84 (0.83)	-
	8 -	-	80 (0.80)	48 (0.67)	112 (0.86)
	9 -	-	-	-	126 (0.86)
	10 -	-	-	60 (0.67)	140 (0.86)
	11 -	-	-	-	154 (0.86)

() Signifies value corresponding to optimal pole-arc to pole-pitch ratio

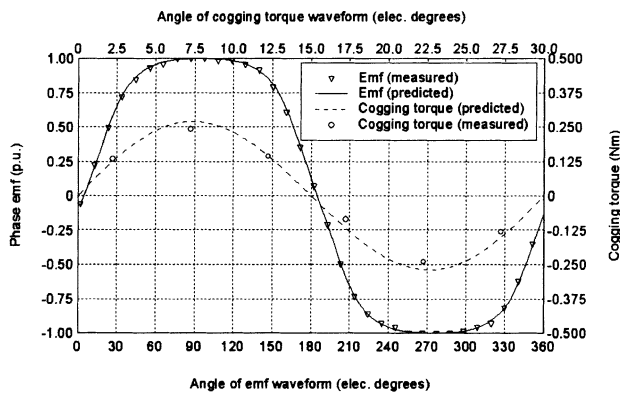


Fig. 2. Comparison of predicted and measured cogging torque waveform for six-phase modular machine.

and have been chosen from a number of one coil per phase modular machine variants. Two-dimensional finite-element analysis has been employed to predict the EMF and cogging torque waveforms of the four-phase, five-phase, and six-phase machines and their one coil per phase variants. The machines with the same number of phases have the same stators, the same air-gap length and the same magnet thickness and magnetization distribution. Fig. 2 compares predicted and measured EMF and cogging torque waveforms for the six-phase machine, shown in Fig. 1(c), where it can be seen that a good agreement exists.

Tables II–IV show the peak cogging torque, as a percentage of the rated torque, the total harmonic distortion (THD) in the EMF, and the EMF fundamental for the four-phase, five-phase, and six-phase machines and their one coil per phase design variants, respectively, when employing one magnet per pole as well as two magnets per pole, each being half the axial length of the rotor, and displaced by half the period of the cogging torque waveform, Fig. 3. In addition, only the EMF harmonics, which contribute to the generation of torque ripple when the machine is supplied by sinusoidal phase current waveforms, are considered in the THD. It can be seen that since for the four-phase designs all EMF harmonics contribute to the generation of torque ripple, these exhibit large THDs in the EMF. Thus, a four-phase design may not be suitable for applications where

TABLE II
PEAK COGGING TORQUE, THD, AND EMF FUNDAMENTAL—FOUR-PHASE MACHINE

Number of pole-pairs	Number of magnets per pole	Peak cogging torque (%)	THD in emf (%)	Emf fundamental (p.u.)
3	1	3.47 (0.08)	3.75 (4.99)	1.00 (0.94)
	2	1.03 (0.38)	1.52 (2.54)	0.98 (0.92)
5	1	4.55 (0.36)	8.81 (5.27)	1.01 (0.94)
	2	0.26 (0.17)	7.44 (4.46)	0.99 (0.92)

() Signifies value corresponding to optimal pole-arc to pole-pitch ratio.

TABLE III
PEAK COGGING TORQUE, THD, AND EMF FUNDAMENTAL—FIVE-PHASE MACHINE

Number of pole-pairs	Number of magnets per pole	Peak cogging torque (%)	THD in emf (%)	Emf fundamental (p.u.)
4	1	4.52 (0.66)	4.72 (1.92)	1.00 (0.96)
	2	0.36 (0.07)	0.75 (0.66)	0.99 (0.95)
6	1	1.86 (0.09)	0.21 (0.12)	0.99 (0.94)
	2	0.06 (0.04)	0.04 (0.02)	0.98 (0.93)
7	1	1.01 (0.06)	0.16 (0.09)	0.82 (0.78)
	2	0.02 (0.01)	0.03 (0.02)	0.81 (0.77)
8	1	0.46 (0.04)	0.22 (0.10)	0.58 (0.56)
	2	0.00 (0.00)	0.04 (0.02)	0.57 (0.55)

() Signifies value corresponding to optimal pole-arc to pole-pitch ratio.

TABLE IV
PEAK COGGING TORQUE, THD, AND EMF FUNDAMENTAL—SIX-PHASE MACHINE

Number of pole-pairs	Number of magnets per pole	Peak cogging torque (%)	THD in emf (%)	Emf fundamental (p.u.)
4	1	5.54 (1.69)	11.22 (10.0)	1.00 (0.86)
	2	1.81 (0.30)	8.68 (7.64)	0.99 (0.85)
5	1	1.24 (0.02)	1.38 (1.77)	1.09 (0.95)
	2	0.02 (0.01)	1.01 (1.30)	1.08 (0.94)
7	1	0.34 (0.07)	1.38 (0.67)	1.03 (0.99)
	2	0.00 (0.00)	1.10 (0.53)	1.02 (0.98)
8	1	3.98 (0.69)	2.91 (1.85)	0.89 (0.79)
	2	0.11 (0.01)	2.31 (1.45)	0.88 (0.78)
10	1	2.64 (0.35)	1.00 (0.45)	0.48 (0.43)
	2	0.03 (0.01)	0.80 (0.36)	0.48 (0.43)

() Signifies value corresponding to optimal pole-arc to pole-pitch ratio.

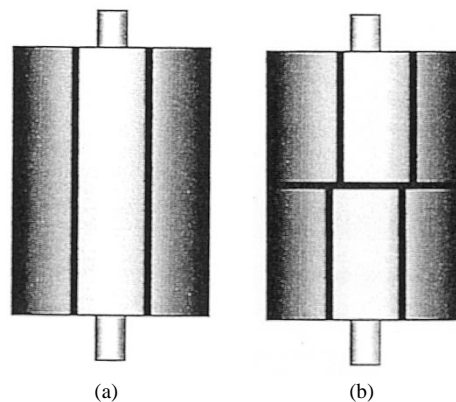


Fig. 3. Schematics of magnet arrangements. (a) One magnet per pole. (b) Two magnets per pole.

a servo characteristic is required. It can also be seen that some slot number and pole number combinations of five-phase and

six-phase design variants would exhibit excellent servo characteristics simply by choosing an optimal pole-arc-to-pole-pitch ratio and/or choosing two magnets per pole, with a negligible loss in torque capability.

The combinations of 10-slot and 8-pole/12-pole, for the five-phase option, and 12-slot and 10-pole/14-pole, for the six-phase option, represent an optimum in the one coil per phase modular machine category.

IV. OPTIMAL TORQUE CONTROL STRATEGY

For an m -phase modular permanent-magnet machine equipped with a surface-mounted magnet rotor, the electromagnetic torque T_e which results when a fault occurs on phase k , is given by

$$T_e = \sum_{j \neq k}^m a_j(\theta) i_j + \begin{cases} 0, & \text{for an open-circuit fault} \\ a_k(\theta) i_k, & \text{for a short-circuit fault} \end{cases} \quad (4)$$

where i_j is the instantaneous current in phase j , and $a_j(\theta) i_j = p(d\psi_j/d\theta) i_j$ is the instantaneous torque of phase j at a given rotor angular position θ , where ψ_j is the magnet flux linkage with phase j and p is the number of pole-pairs, and similarly for the faulted phase k . In the above discussion, a winding short-circuit fault at the terminals is considered. In the case of a partial, inter-turn short circuit, the resulting current in the shorted turns will be much greater than that which results with the terminal short circuit. The controller must immediately short the terminals via the power converter in order to bring the current in the shorted turns back to the level of the short-circuit current at the terminals, upon the detection of the shorted turn fault [15]. The subsequent optimal torque control, therefore, deals with the case of a winding short circuit at terminals. For a given torque demand T_d , the optimal instantaneous currents in the healthy phases can be determined by minimizing a cost function F defined as

$$F = \sum_{j \neq k}^m (L i_j + w \psi_j)^2 \quad (5)$$

subject to the following:

$$T_d = \sum_{j \neq k}^m a_j(\theta) i_j + T_r \quad (6)$$

and current and voltage constraints where w is a weighting factor which is dependent on the speed and torque demand, L is the self-inductance of each phase, and T_r given by

$$T_r = \begin{cases} 0, & \text{for an open-circuit fault} \\ a_k(\theta) i_k, & \text{for a short-circuit fault} \end{cases} + T_{cg}(\theta) \quad (7)$$

represents the uncontrollable torque ripple caused by a winding fault and the cogging torque, $T_{cg}(\theta)$, which may still exist even if all the design parameters mentioned previously have been optimized. A closed-form solution for the above optimization may be obtained using the quadratic programming technique. First, considering the torque demand of (6), and introducing a La-

grange multiplier λ , the augmented cost function F_a is given by

$$F_a = \sum_{j \neq k}^m (L i_j + w \psi_j)^2 + \lambda \left[T_d - \sum_{j \neq k}^m a_j(\theta) i_j - T_r \right]. \quad (8)$$

At the optimal solution, the cost function F_a must satisfy

$$\frac{\partial F_a}{\partial \lambda} = 0 \quad \frac{\partial F_a}{\partial i_j} = 0, \quad j = 1, 2, \dots, m, j \neq k. \quad (9)$$

Substituting (8) into (9), and solving for i_j yields the instantaneous phase currents given by

$$i_j = \frac{a_j(\theta) \left[T_d - T_r + \left(\frac{w}{L} \right) \sum_{j \neq k}^m a_j(\theta) \psi_j \right]}{\sum_{j \neq k}^m [a_j(\theta)]^2} - \frac{w}{L} \psi_j. \quad (10)$$

When current and voltage limits are taken into account, a simple algorithm can be used to adjust the results in (10). By way of example, assuming the current in a healthy phase l reaches the current limit $\pm I_{\max}$, the maximum torque contribution from this phase is

$$T_l = \pm a_l(\theta) I_{\max}. \quad (11)$$

The remaining phases are treated as a new subset, and their optimal current demands are determined in a similar manner as previously described. Thus,

$$i_j = \frac{a_j(\theta) \left[T_d - T_l - T_r + \left(\frac{w}{L} \right) \sum_{j \neq k, l}^m a_j(\theta) \psi_j \right]^2}{\sum_{j \neq k, l}^m [a_j(\theta)]^2} - \frac{w}{L} \psi_j, \quad j \neq k, l. \quad (12)$$

The new set of current demands i_j are checked to identify if any phase current reaches its limit. This process is repeated until all the current demands satisfy the current limit constraint. The voltage limit constraint can be dealt with in a similar manner.

As will be seen from (5), the weighting factor w dictates the amount of flux-weakening effect in the optimization process. Below the base speed Ω_b , which is defined as the maximum speed at which the drive system can produce rated smooth torque without flux weakening, the weighting factor w is set to zero. Therefore, the objective function becomes $L^2 \sum i_j^2$, which is equivalent to minimizing the copper loss $R \sum i_j^2$. Above the base speed, w is a nonzero positive number, which specifies the magnitude of the flux weakening, and varies as a function of both the speed Ω and the torque demand T_d in a manner given by

$$w = \left[\frac{(\Omega - \Omega_b)}{\Omega} \right] \times \frac{T_d}{T_{er}} \quad (13)$$

where T_{er} is the rated torque at the base speed Ω_b . The optimization is, therefore, weighted to minimize the copper loss and the

TABLE V
PARAMETERS OF FOUR-PHASE FAULT-TOLERANT PERMANENT-MAGNET MACHINE

Emf (mV/rad, fundamental)	Phase inductance (mH)	Phase resistance (mΩ)
98.4	0.136	31.61

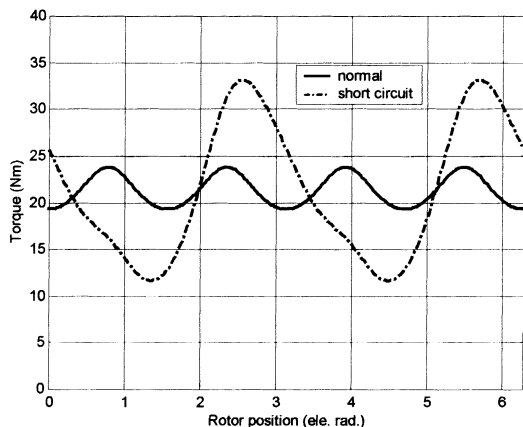


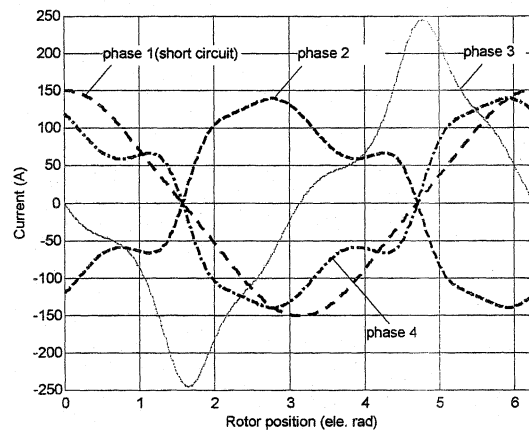
Fig. 4. Variation of torque as a function of rotor position under normal and short-circuit conditions with conventional control strategy.

total flux linkage. As a result, the back EMF is decreased by the effect of flux weakening, and the machine can deliver smooth torque throughout the constant-power operating region.

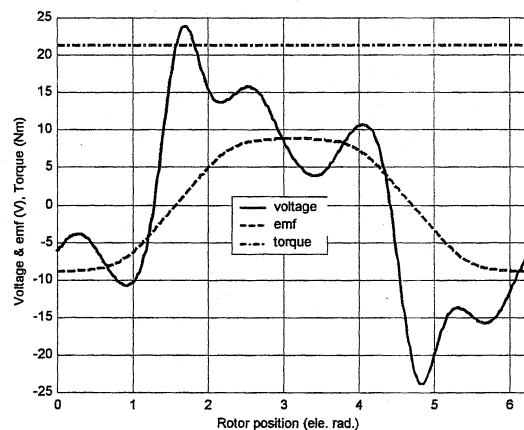
V. SIMULATION RESULTS

The proposed optimal torque control strategy has been implemented by computer simulation on a four-phase, 8-slot, 10-pole modular machine, a schematic of which is shown in Fig. 1(a). This machine is chosen because it exhibits the largest EMF harmonics and, hence, is more demanding in order to achieve a torque ripple free operation by means of the optimal torque control strategy developed in Section IV. The fundamental EMF, the phase inductance, and the resistance of the machine are given in Table V.

Each phase is controlled separately from an H-bridge with a dc supply of 45 V. Fig. 4 compares the torque waveform of the healthy four-phase modular machine with that which results when a phase is short circuited, the controller being required to track a set of sinusoidal current commands to produce the rated torque of 21.36 N·m at a rotor speed of 100 rad/s. As will be seen, due primarily to EMF harmonics and the short-circuit fault, 11.3% and 55.1% torque ripples exist under healthy and fault conditions, respectively. However, these torque ripples can be eliminated completely by using optimal torque control. Fig. 5 shows the current, voltage, EMF, and torque waveforms of the four-phase machine which result under the short-circuit fault condition with the proposed control strategy operating in the constant torque region for the same torque demand and rotor speed as in Fig. 4. It is evident that smooth torque is produced at the expense of increased current harmonics and a higher di/dt . The peak phase voltages which are required to realize these current trajectories also appear to be much higher than those under a normal operation condition. However, with w being set to zero,



(a)



(b)

Fig. 5. Current, voltage, EMF, and torque waveforms under short-circuit condition with proposed control strategy operating in constant torque region at rotor speed of 100 rad/s. (a) Phase currents. (b) Voltage, EMF (in a healthy phase), and torque.

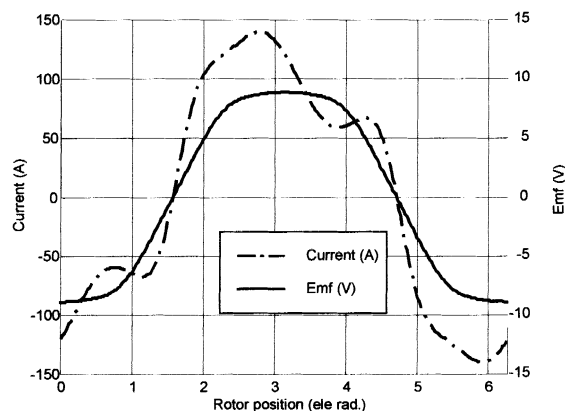


Fig. 6. Variation of phase-2 current and EMF as a function of rotor position under short-circuit condition with proposed control strategy.

the optimal solution minimizes the copper loss $R \sum i_j^2$, with the effect that the phase currents are in phase with their respective EMFs, as illustrated in Fig. 6. Hence, for a fixed dc-link voltage, the maximum speed at which the rated torque can be produced smoothly under a short-circuit fault condition will be much lower than that under healthy conditions.

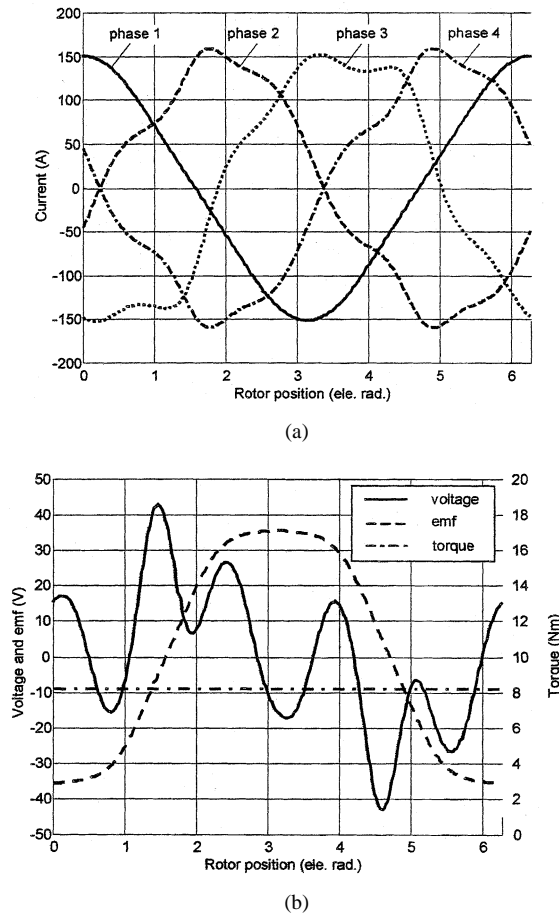


Fig. 7. Current, voltage, EMF, and torque waveforms under short-circuit condition with proposed control strategy operating in constant-power region at rotor speed of 400 rad/s. (a) Phase currents. (b) Voltage, EMF (in healthy phase 2), and torque.

As the rotor speed increases, the available control voltage to realize the required current trajectories becomes progressively less. Therefore, in order to achieve a smooth torque output, it is necessary to introduce a degree of flux-weakening proportional to the speed and torque demand. Fig. 7 shows the current, voltage, EMF, and torque waveforms of the four-phase modular machine under the short-circuit fault condition with the proposed control strategy operating in the constant power region at a rotor speed of 400 rad/s. As can be seen, a ripple-free torque of 8.25 N·m is achieved in the flux-weakening mode even under the short-circuit condition. It is also evident from the phase-2 current and EMF waveforms in Fig. 6(a) and (b) that a significant degree of phase advance in the current with respect to its EMF has been produced to achieve the required flux weakening.

VI. CONCLUSION

The suitability of modular permanent-magnet brushless ac machines for applications in which both a servo characteristic and fault tolerance are required performance attributes has been discussed. It has been shown that optimum combinations of the number of stator slots and the number of rotor poles exist which

enable modular machines to satisfy such requirements under healthy conditions. In addition, a generalized optimal torque control strategy has been described, and shown to produce a ripple-free torque under both healthy and faulted conditions, in both constant-torque and constant-power operating regions.

REFERENCES

- [1] T. Li and G. Slemon, "Reduction of cogging torque in permanent magnet motors," *IEEE Trans. Magn.*, vol. 24, pp. 2901–2903, Nov. 1988.
- [2] B. Ackerman, J. H. Janssen, R. Sottek, and R. I. Van Steen, "A new method for reducing cogging torque in a class of brushless DC motors," *Proc. IEE—Elect. Power Applicat.*, vol. 139, no. 4, pp. 315–338, 1992.
- [3] S. Hwang and D. K. Lieu, "Design techniques for reduction of reluctance torque in brushless permanent magnet motors," *IEEE Trans. Magn.*, vol. 30, pp. 4287–4289, Nov. 1994.
- [4] S. K. Chang, S. Y. Hee, W. N. Ki, and S. C. Hong, "Magnetic pole shape optimization of permanent magnet motor for reduction of cogging torque," *IEEE Trans. Magn.*, vol. 33, pp. 1822–1827, Mar. 1997.
- [5] A. G. Jack, B. C. Mecrow, and J. A. Haylock, "A comparative study of permanent magnet and switched reluctance motors for high-performance fault-tolerant operation," *IEEE Trans. Ind. Applicat.*, vol. 32, pp. 889–895, July/Aug. 1996.
- [6] K. Atallah and D. Howe, "Modular permanent magnet brushless machines for aerospace and automotive applications," in *Proc. 20th Int. Workshop Rare-Earth Magnets and Their Applications*, Sendai, Japan, Sept. 10–14, 2000, p. 1039.
- [7] M. Radaelli, L. Sozzi, and P. Ehrhart, "Novel technologies with PM-machines for ship propulsion," in *Proc. All-Electric Ship Conf.*, 1997, pp. 17–22.
- [8] J. D. Ede, K. Atallah, and D. Howe, "Design variants of modular permanent magnet brushless machines," *J. Appl. Phys.*, vol. 91, pp. 6973–6975, 2002.
- [9] T. Gobalarathnam, H. A. Toliyat, and J. C. Moreira, "Multi-phase fault-tolerant brushless DC motor drives," in *Proc. World Congr. Industrial Applications of Electrical Energy and 35th IEEE-IAS Annu. Meeting*, Rome, Italy, 2000, pp. 1683–1687.
- [10] Z. Q. Zhu and D. Howe, "Influence of design parameters on cogging torque in permanent magnet machines," *IEEE Trans. Energy Conversion*, vol. 15, pp. 407–412, Dec. 2000.
- [11] J. D. Ede, K. Atallah, J. Wang, and D. Howe, "Modular fault-tolerant permanent magnet brushless machines," in *Proc. PEMD2002*, Bath, U.K., 2002, pp. 415–420.
- [12] C. Hanselman, "Minimum torque ripple, maximum efficiency excitation of brushless permanent magnet motors," *IEEE Trans. Ind. Electron.*, vol. 41, pp. 292–300, June 1994.
- [13] C. French and P. Acarnley, "Direct torque control of permanent magnet drives," *IEEE Trans. Ind. Applicat.*, vol. 32, pp. 1080–1088, Sept./Oct. 1996.
- [14] S. Morimoto, Y. Takeda, T. Hirasa, and K. Taniguchi, "Expansion of operating limits for permanent motor by current vector control considering inverter capacity," *IEEE Trans. Ind. Applicat.*, vol. 26, pp. 866–871, Sept./Oct. 1990.
- [15] B. C. Mecrow, A. G. Jack, J. A. Haylock, and J. Coles, "Fault-tolerant permanent magnet machine drives," *Proc. IEE—Elect. Power Applicat.*, vol. 143, no. 6, pp. 437–442, 1996.



Kais Atallah received the Ingenieur d'Etat degree in electrical power engineering from the Ecole Nationale Polytechnique, Algiers, Algeria, and the Ph.D. degree from the University of Sheffield, Sheffield, U.K.

From 1993 to 2000, he was a Research Associate in the Department of Electronic and Electrical Engineering, University of Sheffield, where he is currently a Lecturer. His research interests embrace fault-tolerant permanent-magnet drives for aerospace, magnetic gearing, and "pseudo" direct-drive electrical machines.



Jiabin Wang (M'96) was born in Jiangsu Province, China, in 1958. He received the B.Eng. and M.Eng. degrees from Jiangsu University of Science and Technology, Zhengjiang, China, in 1982 and 1986, respectively, and the Ph.D. degree from the University of East London, London, U.K., in 1996, all in electrical and electronic engineering.

From 1986 to 1991, he was with the Department of Electrical Engineering, Jiangsu University of Science and Technology, where he was appointed a Lecturer in 1987 and an Associate Professor in 1990.

He was a Post-Doctoral Research Associate at the University of Sheffield, Sheffield, U.K., from 1996 to 1997, and a Senior Lecturer at the University of East London from 1998 to 2001. He is currently a Senior Lecturer at the University of Sheffield. His research interests range from motion control to electromagnetic devices and their associated drives.



David Howe received the B.Tech. and M.Sc. degrees from the University of Bradford, Bradford, U.K., in 1966 and 1967, respectively, and the Ph.D. degree from the University of Southampton, Southampton, U.K., in 1974, all in electrical power engineering.

He has held academic posts at Brunel and Southampton Universities, and spent a period in industry with NEI Parsons Ltd., working on electromagnetic problems related to turbogenerators.

He is currently a Professor of Electrical Engineering at the University of Sheffield, Sheffield, U.K., where

he heads the Electrical Machines and Drives Research Group. His research activities span all facets of controlled electrical drive systems, with particular emphasis on permanent-magnet excited machines.

Prof. Howe is a Chartered Engineer in the U.K., and a Fellow of the Institution of Electrical Engineers, U.K.